

Protein Kinase D1 promotes the survival of Random-pattern Skin Flaps in Rats

Jianpeng Chen¹, Hongyu Chen¹, Tao Han¹, Dupiao Zhang¹, Baolong Li¹, Xijie Zhou¹, and Feiya Zhou²

¹Wenzhou Medical College

²Affiliation not available

April 16, 2024

Abstract

Background: Random-pattern skin flaps are often utilized to cover numerous skin defects that can occur for a variety of causes, although tissue ischemia is the most prevalent consequence that leads to surgery failure. Protein Kinase D1 (PKD1), a calcium/calmodulin-dependent serine/threonine kinase, has been linked to angiogenesis and has been shown to protect against ischemic cardiovascular disease in several studies. However, no relevant studies on skin flaps have been recorded. **Methods:** Sixty male Sprague-Dawley rats were randomly separated into control, PKD1, and CID755673 group. We observed postoperative survival, laser Doppler and lead oxide/gelatin angiography were used to assess blood flow, HE (hematoxylin and eosin) staining was used to observe neovascularization, and determined the level of related protein expression through Immunoblotting and immunohistochemistry. **Results:** The PKD1 group has the largest survival area and the most abundant blood supply. The level of angiogenesis and oxidative stress is the highest, and the level of apoptosis is the lowest. The CID755673 group is the opposite. **Conclusion:** The findings show that PKD1 increases the flap's survival rate and is linked to increased angiogenesis, reduced oxidative stress, and apoptosis inhibition.

Introduction

Due to its convenience and flexibility, skin flap has become an ideal material for the repair of all tissue defects in plastic and reconstructive surgery¹⁻³. Although the blood circulation of the random pattern flap is not specific, and distal flap necrosis is the most common postoperative complication⁴. it is mostly utilized to rebuild skin defects related to congenital disorders, trauma, diabetes, and cancer-associated abnormalities. If the flap length-to-width ratio exceeds 2:1, the distal portions become liable to necrosis, thus limiting its clinical use⁵. Angiogenesis is a critical factor in skin flaps survival; hence, adequate angiogenesis is a guarantee of flap survival following reconstructive surgery⁶. Oxidative stress and apoptosis are key contributors in skin flap necrosis in previous studies⁷. Suppressing necrosis of skin flaps requires lowering oxidative stress, inhibiting apoptosis, and preventing ischemia-reperfusion (I/R) injury^{8,9}. To improve random skin flap survival, medical treatments that reduce oxidative stress and apoptosis and stimulate angiogenesis might be a suitable choice.

PKD1, also known as PKC- μ , is a serine/threonine kinase that is a PKD family member, which is a calcium/calmodulin-dependent kinase (CaMK) family subgroup¹⁰. It can function on various pathways and is involved in controlling a variety of biological processes^{11,12}. PKD1 is a critical regulator of tumor angiogenesis, promoting the development of new blood vessels effectively¹³. PKD1 has been shown in some studies to protect cardiomyocytes from damage caused by regional myocardial ischemia and hypoxia¹⁴⁻¹⁶. However, the effects of PKD1 on flaps are unknown.

CID755673 is a PKD1-specific inhibitor that was employed in the current study. Unlike many other kinase inhibitors, CID755673 has a high degree of selectivity due to the presence of the kinase ATP binding domain¹⁷. It has been utilized to suppress the growth and motility of prostate cancer by inhibiting the process of PKD regulation, including class IIa HDAC phosphorylation^{18, 19}. As a result, we hypothesize that PRKD1 (an exogenous recombinant PKD1) may reduce oxidative stress, increase angiogenesis, and prevent cellular apoptosis, leading to the enhancement of random flap survival.

Materials and Methods

Animals and ethics statement

Wenzhou Medical University provided us with 250–300 g sixty male Sprague-Dawley (SD) rats. All experiments and animal care were done following the Guide for the Care and Use of Laboratory Animals of the China National Institutes of Health and approved by the Animal Care and Use Committee of Wenzhou Medical University (wydw2019-0954). SD rats were placed within a suitable environment with a twelve-hour light/dark cycle and sufficient water and food. Sixty rats were assigned in a random fashion to one group of the following: Control (n= 20), PKD1 (n= 20), or CID755673 (n= 20).

Reagents and antibodies

PKD1 (PRKD1; purity [?]98%) was provided by Carna Biosciences, Inc(USA). The CID755673 was purchased from MedChemExpress LLC (USA). Pentobarbital sodium, hematoxylin and eosin staining kit, lead oxide-gelatin, and diaminobenzidine (DAB) were procured from Solarbio life Science (China). Wuhan Boster Biological Technology, Ltd. and Bioget Technology provided anti-cadherin 5 and anti-GAPDH monoclonal antibodies, respectively. The Proteintech Group (Chicago, USA) provided primary antibodies against GAPDH, HO1, SOD1, MMP9, VEGF, and CASP3. Cell Signaling Technologies (Beverly, Massachusetts) provided antibodies against CYC, eNOS, cadherin 5, and Bax. Santa Cruz Biotechnology Inc. antibody (Dallas, Texas, USA) provided the second goat anti-rabbit IgG. The ECL Plus Reagent kits and the BCA Kits were obtained from PerkinElmer Life Sciences and Beyotime Biotechnology accordingly.

Drug Administration

In physiological saline, PKD1 was dissolved in 2% DMSO. The PKD1 group received daily intraperitoneal injections of PKD1 (10 μ g/kg) for seven days following flap surgery. The control group got the same DMSO saline volume. The CID755673 group was in the same injection mode (5mg/kg of body weight).

Random-Pattern Skin Flap Model

The back hair was removed, and all rats were intraperitoneally anesthetized with 40 mg/kg of 2% (w/v) sodium pentobarbital. By cutting the skin along a specified line (3cm \times 9cm), random skin flaps were created. The skin was cut along the design line, and the skin flap underwent entire separation from the deep fascia. The bilateral sacral arteries were cut off and finally sutured in situ intermittently with 4-0 sutures. Each flap had three equal zones: zone I (proximal), zone II (intermediate), and zone III (distal) (**Figure 1**).

Flap Survival Assessment

We assessed the color, appearance, texture, hair condition, and necrosis of the skin flap on the third and seventh days post-surgery. Survival status was determined using photographs, and, using ImageJ software, the survival area range/total area \times 100% was considered as the survival area percentage.

Tissue edema evaluation

To determine tissue edema degree, we measured the water content of the tissue. On the seventh day after surgery and from each group, six skin flaps were weighed, deposited at 50°C in an autoclave for dehydration, and re-weighed until a constant weight was maintained for 48 hours at least. $([\text{wet weight} - \text{dry weight}]/\text{wet weight}) \times 100\% = \text{water content percentage} (\%)$.

Laser Doppler Blood Flow Imaging

Six rats from each group were anesthetized and, on the third and seventh postoperative days, the flap blood flow was assessed utilizing laser Doppler blood flow imaging. For quantification of flap blood flow and the indicators, the Moor LDI Review software was employed.

Lead Oxide Angiography

The rats (n=6) were injected with lead oxide gelatin (80mL/kg) through the carotid artery on the seventh POD until the limbs became orange. The perfused rats were then refrigerated at -80°C overnight. The skin flaps were totally removed, and the blood vessels were seen using an X-ray machine (54kVp, 40mA, 100s exposure) following thawing in the next day.

Hematoxylin and Eosin Staining

At the 7th POD, six tissue specimens from the flap II region (central tissue) measuring 1cm × 1cm were collected after the rats were sacrificed with an excess sodium pentobarbital dose. After 24 hours of fixation in 4% (v/m) paraformaldehyde, these specimens were embedded in paraffin wax and transversely sectioned (4 mm thickness). We randomly selected the number of blood vessel cross-sections per unit area in different fields of view (/mm²) under the microscope (Olympus Corp, Japan) to compute the mean blood vessel density of the flap tissue in order to evaluate the microcirculation level.

Immunohistochemistry

From each group, six randomly selected samples underwent deparaffinization using xylene and were rehydrated with a graded ethanol series. Endogenous peroxidase was blocked with a 3% hydrogen peroxide solution after washing. It was then buffered with sodium citrate to facilitate antigen retrieval (10.2 mM, 20 min, 95°C). Using PBS containing 10% (w/v) bovine serum albumin, the sample was blocked for 10 minutes, and then at 4°C with a target of cadherin 5 (1: 200), SOD1 (1: 100), CD34 (1: 100), CASP3 (1: 200), or VEGF (1: 200). After that, the slide underwent incubation at room temperature for two hours with the corresponding HRP-conjugated secondary antibody (1:1000). Following washing, DAB dyeing, and counterstaining with hematoxylin was accomplished. A microscope was utilized to collect images for further analysis from at least six random fields of view (Olympus Corp., Japan).

Immunoblotting

At POD7, the rats were sacrificed. From area II, six 0.5×0.5 cm samples were collected for western blot analysis. To extract the flap tissue protein, lysis buffer was utilized, and using the BCA assay, concentration was determined. PAGE (12%) was used to separate the protein, which was then transferred to the PVDF membrane. At room temperature and after 2 hours and using 5% (w/v) nonfat milk, the membrane was blocked, then underwent incubation with the primary antibody VEGF (1: 1000), eNOS (1: 1000), MMP9 (1: 1000), HO1 (1: 1000), cadherin 5 (1: 500), Bax (1: 500), SOD1 (1: 1000), CYC (1: 1000), caspase 3 (CASP3) (1: 1000), and GAPDH (1: 1000) at 4°C overnight, then at room temperature, it underwent re-incubation with HRP-conjugated IgG secondary antibody for two hours. To visualize the membrane, the ECL reagent kit was employed. To assess the blots intensity, the Image Lab 3.0 software was utilized.

Statistical analyses

Using SPSS software (version 22.0; Chicago, Illinois, USA), data analysis was done. Means ± standard error of the mean was used to summarize all data. Using the independent-sample t-test, the two groups means were compared. A p-value <0.05 was statistically significant.

Result

3.1PKD1 significantly enhanced random skin flap survival

On day three postoperative, the skin flaps in area III began to become necrotic, turn black, dry, wrinkled, and rigid. Among the three groups, the flap survival area showed significant differences. Significant changes

became apparent on the seventh POD. In the PKD1 group, the survival area was larger compared to the control group ($58.40 \pm 2.28\%$ VS $76.11 \pm 0.74\%$, $P < 0.01$). Compared to the control group, the flap survival rate was significantly lower in the CID755673 group ($58.40 \pm 2.28\%$ VS $40.56 \pm 1.01\%$, $P < 0.01$) (**Figure 2 A, B**).

To determine the degree of edema, the inner side of flap tissues of three groups were observed. The control group had a considerably greater water content in the flap than the PKD1 group ($48.67 \pm 1.31\%$ VS $37.83 \pm 1.33\%$, $p < 0.01$), and the CID755673 group had the greatest water content ($48.67 \pm 1.31\%$ VS $58.93 \pm 1.24\%$, $p < 0.05$) (**Figure 2 C, D**).

The intensity of the blood flow signal was significantly stronger in the PKD1 group than in the control group on the 3rd ($224.40 \pm 7.70\text{PU}$ VS $289.50 \pm 14.92\text{PU}$, $P < 0.01$) and 7th PODs ($346.60 \pm 10.02\text{PU}$ VS $431.50 \pm 21.97\text{PU}$, $P < 0.01$). The CID755673 group is the worst on the 3rd ($224.40 \pm 7.70\text{PU}$ VS $172.80 \pm 8.07\text{PU}$, $p < 0.05$) and 7th PODs ($346.60 \pm 10.02\text{PU}$ VS $279.40 \pm 2.78\text{PU}$, $p < 0.05$) (**Figure 2 F, G**). New blood vessels number was significantly larger in the PKD1 group than in the control group as regards the lead oxide gelatin angiography. (**Figure 2 E**). Compared to the control group, all the above results were significantly worse in the CID group. Overall, the findings demonstrate that PKD1 can improve random flaps survival.

3.2 PKD1 improves angiogenesis in random skin flap

The vessel density was assessed by H&E staining, and CD34-positive vessels were calculated under IHC. The results of HE were significantly higher in the PKD1 group ($128.50 \pm 3.60/\text{mm}^2$) compared to the control group ($76.83 \pm 4.40/\text{mm}^2$) ($p < 0.01$). In contrast, the CID755673 group ($43.17 \pm 2.75/\text{mm}^2$) showed lower results ($P < 0.01$). (**Figure 3 A, B**).

The number of CD34-positive vessels was $68.63 \pm 4.54/\text{mm}^2$ in the control group, $125.00 \pm 5.51/\text{mm}^2$ in the PKD1 group, and $35.50 \pm 2.09/\text{mm}^2$ in the CID755673 group. The experimental and control groups demonstrated significant differences ($p < 0.01$), as well as the control and CID755673 groups ($p < 0.05$) (**Figure 3 C, D**).

Adequate blood supply, as determined by angiogenesis, can increase flap survival. As a result, immunohistochemistry and western blot were utilized for determining the expression levels of neovascularization markers. IHC analysis of VEGF and cadherin5 expression revealed that, compared to the control group, PKD1 group results were significantly higher; whereas results in the CID755673 group were significantly lower (Figure 3 F, H) (VEGF and cadherin5: control vs. PKD1, $p < 0.01$; control vs. CID755673, $p < 0.01$). Additionally, VEGF and cadherin5 protein expression levels were increased in PKD1, as showed by western blot analysis, while MMP9 and CID755673 protein expression levels were decreased (VEGF, MMP9, and cadherin 5: control vs. PKD1, $p < 0.05$; control vs. CID755673, $p < 0.01$) (**Figure 3 I, J**).

3.3 PKD1 Attenuates Apoptosis in random skin flap

Skin flap necrosis is associated with apoptosis. Thus, we used immunohistochemistry to determine the level of CASP3 and found that CASP3 staining was significantly reduced in the dermis of PKD1-treated rats than the control group. A significantly higher prevalence was noted in the CID755673 group (control vs PKD1, $p < 0.01$; control vs CID755673, $p < 0.01$) (**Figure 4 A, B**). The underlying results were consistent with the western blot findings. Additionally, immunoblotting for Bax and CYC revealed that the PKD1 group showed significantly lower levels of CYC and Bax than the control group. Similarly, the CID755673 were higher (CYC and CASP3: control vs PKD1, $p < 0.01$; control vs CID755673, $p < 0.05$; Bax: control vs PKD1, $p < 0.05$; control vs CID755673, $p < 0.01$)

(**Figure 5 C, D**).

3.4 PKD1 Attenuates Oxidative Stress in random skin flap

In skin flap necrosis development, oxidative stress is a critical factor. We used IHC and Western blot to determine oxidative stress-related proteins. According to IHC results, the PKD1 group showed a significantly

higher SOD1 level in the dermis compared to the control group (control vs. PKD1, $p < 0.01$; control vs. CID755673, $p < 0.01$) (**Figure 5 A, B**). We also measured eNOS, SOD1, and HO1 expression levels in the flaps by western blot. In the PKD1 group, these proteins expression was significantly upregulated than the control group, while all the above lowest results were observed in the CID755673 group (SOD1, HO1, and eNOS: control vs. PKD1, $p < 0.01$; control vs. CID755673, $p < 0.01$)

(**Figure 5 C, D**).

Discussion

As a stress-activated serine/threonine kinase, protein kinase D1 is crucial in various fundamental physiological and biological functions, including cell growth, apoptosis, adhesion, motility, and angiogenesis^{16, 20, 21}. Because of the low axial blood flow and IR, distal skin flap necrosis is a frequent postoperative complication^{6, 22}. As a result, the axial vascular distribution must be carefully considered. The perfusion pressure of the flap blood and the nascent capillaries is critical for flap survival²³. As a result, PKD1 may be able to increase the random flaps survival rate. Our findings indicate that PKD1 can enhance random skin flap survival through inhibiting oxidative stress and apoptosis and increasing distal flap neovascularization.

According to some studies, angiogenesis is crucial for random skin flaps survival^{7, 24}. Angiogenesis entails a number of complex processes, including preexisting cell connections destruction, endothelial cell sprouting, mitosis, and maturation of new capillaries²⁵. According to some studies, VEGF is required for endothelial cell mitosis and can increase microvascular permeability^{26, 27}. By integrating VEGF-A signaling and interacting with the extracellular matrix, PKD1-regulated alphavbeta3 transport promotes angiogenesis²⁸. Increasing evidence indicates that the PKD1-mediated signaling pathway is vital for endothelial cells, particularly in VEGF-induced angiogenesis regulation²⁹⁻³¹. It is a critical signal for angiogenesis³². MMP9 is involved in the angiogenic switch and can aid in VEGF release³³. Cadherin 5 prevents the formation of disorganized endothelial aggregates in new blood vessels and forms intercellular junctions³⁴. According to IHC and western blotting analysis, PKD1 treatment increased Cadherin 5 and VEGF expression in stromal cells and blood vessels in the dermis. The present study demonstrated that PKD1 stimulates new blood vessels formation and increases microvessels number in ischemic skin flaps, thereby increasing the regenerated blood vessels number and quality. Thus, we hypothesize that PKD1 promotes neovascularization in the flap's dermis by increasing VEGF, cadherin 5, and MMP9 levels.

When the flap's blood supply is restored, the tissue may experience I/R damage and produce an abnormal amount of reactive oxygen species (ROS)⁸, finally resulting in necrosis in the flap's distal region³⁵. PKD1 protects cells from oxidative stress and minimizes hypoxia-induced damage³⁶. Additionally, PKD1 regulates the detoxification of reactive oxygen and nitrogen species in the mitochondria, leading to cells protection against oxidative stress^{37, 38}. Cell survival and cell death in dopaminergic neuronal cells are regulated by the PKD1-mediated protective mechanism³⁸. SOD is a well-known antioxidant enzyme that converts superoxide radicals to hydrogen peroxide³⁹. The PKD1-induced protective signaling pathways are hypothesized to be involved in the manipulation of mROS effects and age-related diseases associated with mitochondrial dysfunction^{40, 41}. HO1 and eNOS are both involved in the process of oxidative stress and have antioxidant properties⁴². As a result, we predicted that PKD1 could help improve flap survival by inhibiting oxidative stress. IHC and WB analysis revealed that PKD1 enhanced eNOS, SOD1, and HO1 expression, all of which are considered to reduce oxidative stresses. Thus, our findings indicated that PKD1 inhibited oxidative stress and subsequently alleviated IRI in random skin flaps.

During flap I/R injury, the primary mode of cell death is apoptosis⁴³. PKD1 acts as a critical anti-apoptotic kinase, protecting neuronal cells from oxidative stress throughout the early phases. Dopaminergic neuronal cells subjected to H₂O₂ or 6-OHDA caused phosphorylation of the PKD1 activation loop (PKD1S744E/748E) long before neuronal cell death was induced³⁸. Numerous cellular stressors stimulate the apoptotic pathway (mitochondria-mediated), causing a mitochondrial release of CYC, which in turn leads to activation of the caspase cascade and ultimately CASP3⁴⁴. Bax considerably increases the outer mitochondrial membrane permeability during cell death, resulting in mitochondrial swelling⁴⁵. We investigated CASP3, CYC, and Bax

expression levels in response to various treatments to assess apoptosis extent. The PKD1 group suppressed the expression of CASP3, Bax, and CYC, according to western blotting analysis. A significantly lower CASP3 expression was noted in the PKD1 group than the control group, showing that PKD1 attenuated apoptosis levels in ischemic skin flaps.

The worst results were reported in the CID755673 group, which may indicate that PKD1 improves the prognosis and survival rate of skin flaps.

Conclusion

The PKD1 inhibits oxidative stress and apoptosis and promotes angiogenesis, hence increasing random flaps survival rate. Further research is required to determine whether PKD1 has a beneficial effect on clinical flap surgery patients. Also, the underlying mechanism differences between endogenous and exogenous PKD1 should be validated.

Acknowledgments

This study was supported by Wenzhou Science and Technology Bureau program (Y2020982).

Conflicts of Interest

The authors declare no conflicts of interest.

Data availability Statement:

The data used to support the findings of this study are available from the corresponding author upon request.

Abbreviations

- 6-OHDA 6-hydroxydopamine
- ATP Adenosine triphosphate
- BCA Bicinchoninic acid
- CASP Caspase
- CYC Cytochrome C
- DAB Diaminobenzidine
- DMSO Dimethyl sulfoxide
- eNOS endothelial nitric oxide synthase
- H&E Hematoxylin and eosin
- HDAC Histone deacetylase
- HO Heme oxygenase
- IHC Immunohistochemical
- Ip Intraperitoneal
- IRI Ischemia-reperfusion injury
- LDF Laser Doppler flowmeter
- MMP Matrix metalloproteinase
- MVD Mean vessel density
- PBS Phosphate-buffered saline
- PKC Protein kinase C
- PKD1 Protein kinase D1
- POD Post-operation day
- PRKD1 Protein recombinant kinase D1
- PU Perfusion units
- ROS Reactive oxygen species
- SEM Standard Error of Mean
- SOD Superoxide dismutase
- VEGF Vascular endothelial growth factor
- WB Western blotting

References

1. Yan H, He Z, Li Z, et al. Large Prefabricated Skin Flaps Based on the Venous System in Rabbits: A Preliminary Study. *Plastic and Reconstructive Surgery* 2013; 132: 372E-80E.
2. Shandalov Y, Egozi D, Koffler J, et al. An engineered muscle flap for reconstruction of large soft tissue defects. *Proceedings of the National Academy of Sciences of the United States of America* 2014; 111: 6010-15.
3. Angrigiani C, Rancati A, Artero G, Khouri RK, Jr., Walocko FM. Stacked Thoracodorsal Artery Perforator Flaps for Unilateral Breast Reconstruction. *Plastic and Reconstructive Surgery* 2016; 138: 969E-72E.
4. Chen G, Shen HG, Zang LL, et al. Protective effect of luteolin on skin ischemia-reperfusion injury through an AKT-dependent mechanism. *International Journal of Molecular Medicine* 2018; 42: 3073-82.
5. Deng C, Wu B, Wei Z, et al. A Systematic Study of Vascular Distribution Characteristics and Axis Design of Various Flap Types. *Medical Science Monitor* 2019; 25: 721-29.
6. Saito I, Hasegawa T, Ueha T, et al. Effect of local application of transcutaneous carbon dioxide on survival of random-pattern skin flaps. *Journal of Plastic Reconstructive and Aesthetic Surgery* 2018; 71: 1644-51.
7. Lin RJ, Chen HW, Callow D, et al. Multifaceted effects of astragaloside IV on promotion of random pattern skin flap survival in rats. *American Journal of Translational Research* 2017; 9: 4161-+.
8. Fukunaga Y, Izawa-Ishizawa Y, Horinouchi Y, et al. Topical application of nitrosonifedipine, a novel radical scavenger, ameliorates ischemic skin flap necrosis in a mouse model. *Wound Repair and Regeneration* 2017; 25: 217-23.
9. Wu HQ, Ding J, Wang L, et al. Valproic acid enhances the viability of random pattern skin flaps: involvement of enhancing angiogenesis and inhibiting oxidative stress and apoptosis. *Drug Design Development and Therapy* 2018; 12: 3951-60.
10. Rykx A, De Kimpe L, Mikhalap S, et al. Protein kinase D: a family affair. *Febs Letters* 2003; 546: 81-86.
11. Wang QMJ. PKD at the crossroads of DAG and PKC signaling. *Trends in Pharmacological Sciences* 2006; 27: 317-23.
12. Jaggi M, Du C, Zhang WG, Balaji KC. Protein kinase D1: a protein of emerging translational interest. *Frontiers in Bioscience-Landmark* 2007; 12: 3757-67.
13. Hollenbach M, Stoll SJ, Jorgens K, Seufferlein T, Kroll J. Different Regulation of Physiological and Tumor Angiogenesis in Zebrafish by Protein Kinase D1 (PKD1). *Plos One* 2013; 8.
14. Zhao D, Wang W, Wang H, et al. PKD knockdown inhibits pressure overload-induced cardiac hypertrophy by promoting autophagy via AKT/mTOR pathway. *International Journal of Biological Sciences* 2017; 13: 276-85.
15. Dai SN, Hou AJ, Zhao SM, et al. Ginsenoside Rb1 Ameliorates Autophagy of Hypoxia Cardiomyocytes from Neonatal Rats via AMP-Activated Protein Kinase Pathway. *Chinese Journal of Integrative Medicine* 2019; 25: 521-28.
16. Avkiran M, Rowland AJ, Cuello F, Haworth RS. Protein kinase D in the cardiovascular system - Emerging roles in health and disease. *Circulation Research* 2008; 102: 157-63.
17. Venardos K, De Jong KA, Elkamie M, Connor T, McGee SL. The PKD inhibitor CID755673 enhances cardiac function in diabetic db/db mice. *PLoS One* 2015; 10: e0120934.
18. Sharlow ER, Giridhar KV, LaValle CR, et al. Potent and selective disruption of protein kinase D functionality by a benzoxoloazepinone. *J Biol Chem* 2008; 283: 33516-26.
19. Yuan J, Liu Y, Tan T, et al. Protein kinase d regulates cell death pathways in experimental pancreatitis. *Front Physiol* 2012; 3: 60.

20. Steinberg SF. Regulation of Protein Kinase D1 Activity. *Molecular Pharmacology* 2012; 81: 284-91.
21. LaValle CR, George KM, Sharlow ER, et al. Protein kinase D as a potential new target for cancer therapy. *Biochimica Et Biophysica Acta-Reviews on Cancer* 2010; 1806: 183-92.
22. Brewer MB, Stump AL, Holton LH, et al. Effects of systemic tadalafil on skin flap survival in rats. *Eplasty* 2012; 12: e45-e45.
23. He JB, Fang MJ, Ma XY, Li WJ, Lin DS. Angiogenic and anti-inflammatory properties of azadirachtin A improve random skin flap survival in rats. *Experimental Biology and Medicine* 2020; 245: 1672-82.
24. Wu H, Ding J, Wang L, et al. Valproic acid enhances the viability of random pattern skin flaps: involvement of enhancing angiogenesis and inhibiting oxidative stress and apoptosis. *Drug Design Development and Therapy* 2018; 12: 3951-60.
25. Nowak-Sliwinska P, Alitalo K, Allen E, et al. Consensus guidelines for the use and interpretation of angiogenesis assays. *Angiogenesis* 2018; 21: 425-532.
26. Brown LF, Yeo KT, Berse B, et al. VASCULAR-PERMEABILITY FACTOR (VASCULAR ENDOTHELIAL GROWTH-FACTOR) IS STRONGLY EXPRESSED IN THE NORMAL-MALE GENITAL-TRACT AND IS PRESENT IN SUBSTANTIAL QUANTITIES IN SEMEN. *Journal of Urology* 1995; 154: 576-79.
27. Shi SR, Xie J, Zhong J, et al. Effects of low oxygen tension on gene profile of soluble growth factors in co-cultured adipose-derived stromal cells and chondrocytes. *Cell Proliferation* 2016; 49: 341-51.
28. di Blasio L, Droetto S, Norman J, Bussolino F, Primo LJT. Protein kinase D1 regulates VEGF-A-induced alphavbeta3 integrin trafficking and endothelial cell migration. *Angiogenesis* 2010; 11: 1107-18.
29. Matthews SA, Liu P, Spitaler M, et al. Essential role for protein kinase D family kinases in the regulation of class II histone deacetylases in B lymphocytes. *Molecular and Cellular Biology* 2006; 26: 1569-77.
30. Ha CH, Wang W, Jhun BS, et al. Protein kinase D-dependent phosphorylation and nuclear export of histone deacetylase 5 mediates vascular endothelial growth factor-induced gene expression and angiogenesis. *Journal of Biological Chemistry* 2008; 283: 14590-99.
31. Ha CH, Jin ZG. Protein kinase D1, a new molecular player in VEGF signaling and angiogenesis. *Molecules and Cells* 2009; 28: 1-5.
32. Okamoto T, Usuda H, Tanaka T, Wada K, Shimaoka M. The Functional Implications of Endothelial Gap Junctions and Cellular Mechanics in Vascular Angiogenesis. *Cancers* 2019; 11.
33. Bergers G, Brekken R, McMahon G, et al. Matrix metalloproteinase-9 triggers the angiogenic switch during carcinogenesis. *Nature Cell Biology* 2000; 2: 737-44.
34. Cao J, Ehling M, Marz S, et al. Polarized actin and VE-cadherin dynamics regulate junctional remodelling and cell migration during sprouting angiogenesis. *Nature Communications* 2017; 8.
35. Cai L, Cao B, Lin D. Effects of Traditional Chinese Medicine Huangqi Injection (Radix astragali) on Random Skin Flap Survival in Rats. *Journal of Reconstructive Microsurgery* 2015; 31: 565-70.
36. Zembrzuska K, Ostrowski RP, Matyja E. Hyperbaric oxygen increases glioma cell sensitivity to antitumor treatment with a novel isothiourea derivative in vitro. *Oncology Reports* 2019; 41: 2703-16.
37. Sundram V, Chauhan SC, Jaggi M. Emerging Roles of Protein Kinase D1 in Cancer. *Molecular Cancer Research* 2011; 9: 985-96.
38. Asaithambi A, Kanthasamy A, Saminathan H, Anantharam V, Kanthasamy AG. Protein kinase D1 (PKD1) activation mediates a compensatory protective response during early stages of oxidative stress-induced neuronal degeneration. *Molecular Neurodegeneration* 2011; 6.

39. Batinic-Haberle I, Tovmasyan A, Roberts ERH, et al. SOD Therapeutics: Latest Insights into Their Structure-Activity Relationships and Impact on the Cellular Redox-Based Signaling Pathways. *Antioxidants & Redox Signaling* 2014; 20: 2372-415.
40. Storz P, Doppler H, Toker A. Protein kinase D mediates mitochondrion-to-nucleus signaling and detoxification from mitochondrial reactive oxygen species. *Molecular and Cellular Biology* 2005; 25: 8520-30.
41. Storz P. Mitochondrial ROS - radical detoxification, mediated by protein kinase D. *Trends in Cell Biology* 2007; 17: 13-18.
42. Fuyuno Y, Uchi H, Yasumatsu M, et al. Perillaldehyde Inhibits AHR Signaling and Activates NRF2 Antioxidant Pathway in Human Keratinocytes. *Oxidative Medicine and Cellular Longevity* 2018: 2018.
43. Rah DK, Min HJ, Kim YW, Cheon YW. Effect of Platelet-Rich Plasma on Ischemia-Reperfusion Injury in a Skin Flap Mouse Model. *International Journal of Medical Sciences* 2017; 14: 829-39.
44. Elmore S. Apoptosis: A review of programmed cell death. *Toxicologic Pathology* 2007; 35: 495-516.
45. Zhou KL, Zhou YF, Wu K, et al. Stimulation of autophagy promotes functional recovery in diabetic rats with spinal cord injury. *Scientific Reports* 2015: 5.

Figure legends

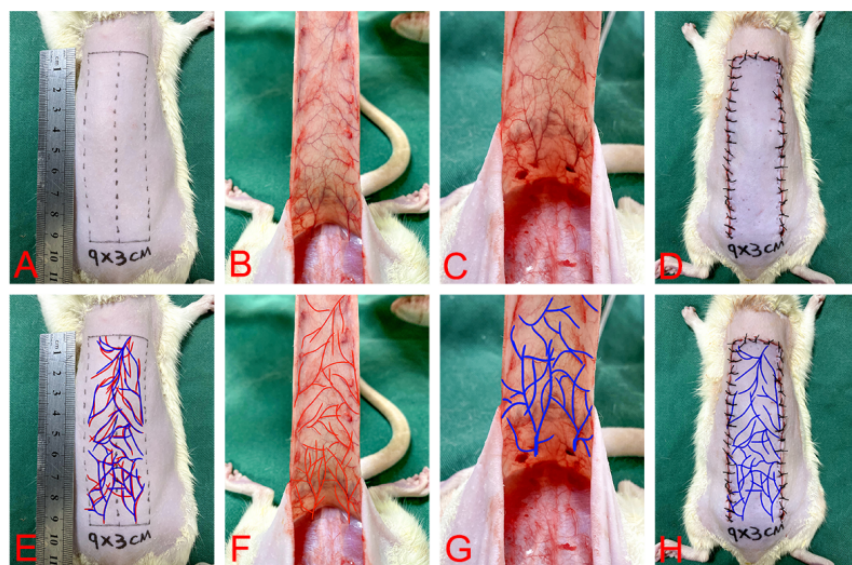


Figure 1: Making a random flap model process A. Design a random 3×9 cm flap in the middle of the back of each rat. B. Separate the sacral arteries. C. Cut both sacral arteries. D. The flap is sutured in situ. E-F. Related vascular network

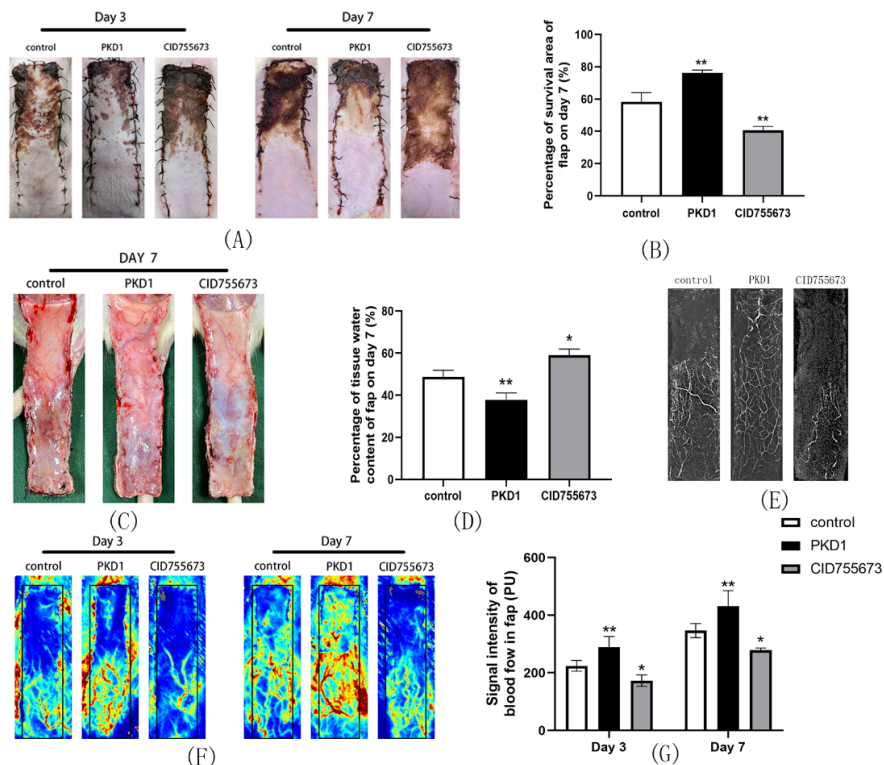


Figure 2: PKD1 promoted the survival of flaps. (A) Flap digital photographs were taken on the third & seventh PODs in the studied groups. (B) Histogram of survival area percentages in each group. (C) POD 7 digital photographs of tissue edema (inner face) in the studied groups. (D) Histogram of the percentage of water content in the skin flap tissue on the seventh PODs. (E) Flap angiography was performed on the seventh PODs in all three groups. (F) LDBF imaging of blood flow in the flap on the third and seventh PODs in the studied groups. (G) Histogram of the quantified blood flow signal intensity on the 3rd and 7th PODs. * $p < 0.05$ and ** $p < 0.01$, vs control group. Mean \pm SEM was used for data presentation, $n = 6$ per group.

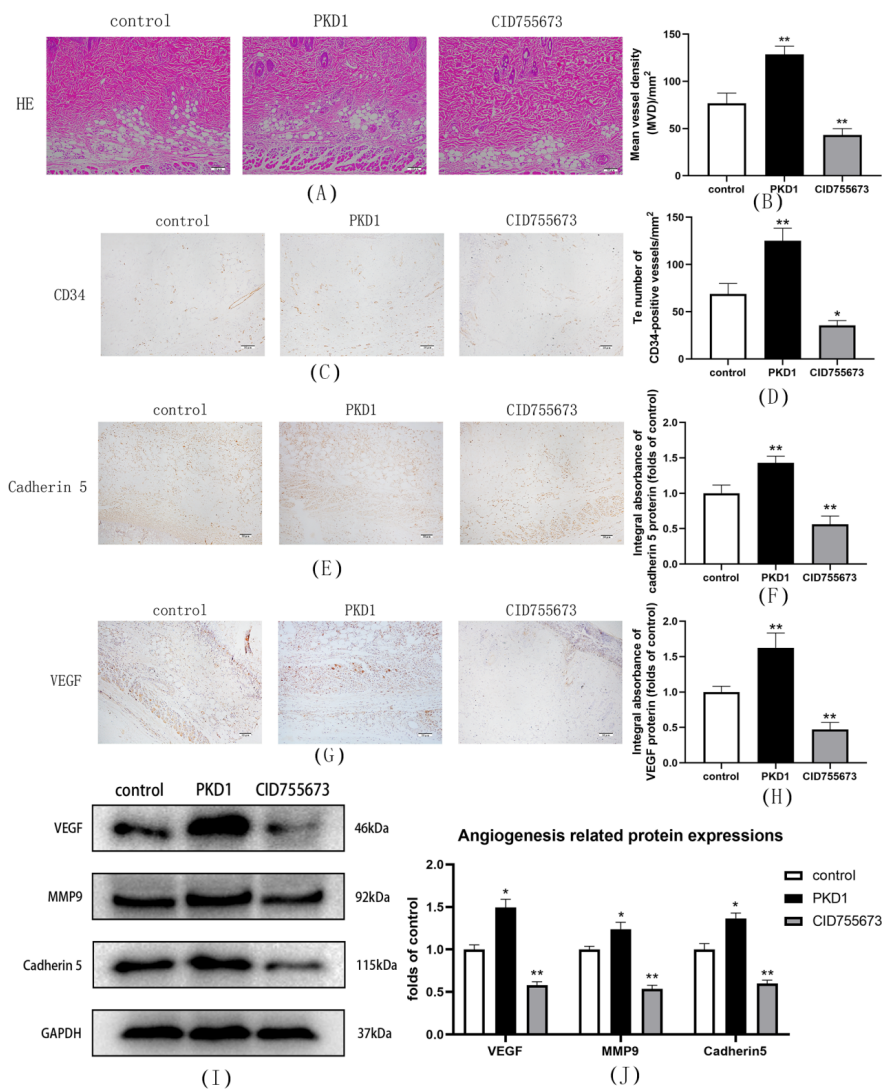


Figure 3: Effect of PKD1 on angiogenesis in the random-pattern skin flaps . (A) Images of H&E staining in each group (original magnification: 200x; scale bar: 50 μm). (B) Histogram of H&E-stained MVD. (C) CD34-positive vessels IHC staining in the studied groups (original magnification: 200x; scale bar: 50 μm). (D) CD34-positive vessel density in all groups. (E, G) IHC staining of VEGF and Cadherin 5 expressions in the flap in the studied groups (original magnification: 200x; scale bar: 50 μm). (F, H) VEGF and Cadherin 5 optical density values in each group. (I) Western blotting analysis of Cadherin 5, MMP9, and VEGF expressions in the studied groups, with GAPDH as an internal control. (J) The optical density values of MMP9, VEGF, and Cadherin 5 in each group. * $p < 0.05$ and ** $p < 0.01$, vs control group. Mean \pm SEM was used for data presentation, $n = 6$ per group.

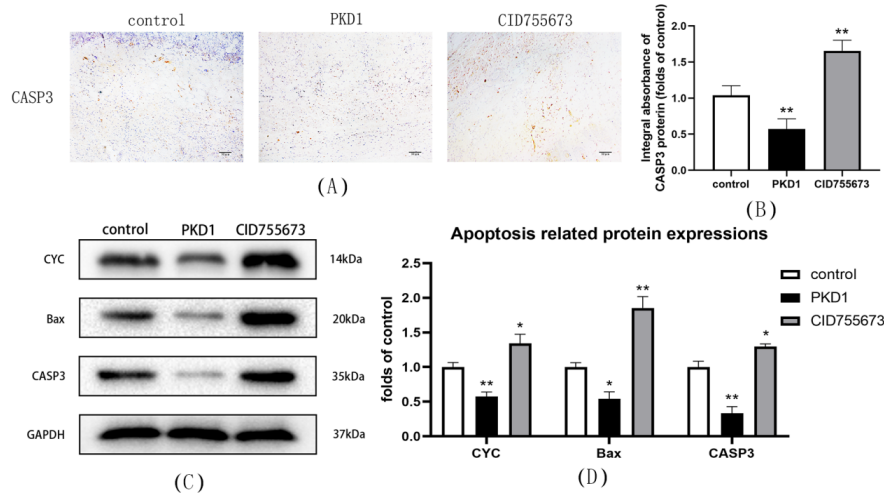


Figure 4: Effect of PKD1 on apoptosis in the random-pattern skin flaps . (A) IHC staining of CASP3 expression in the flap in the studied groups (original magnification: 200×; scale bar: 50 μm). (B) The optical density value of CASP3 in each group. (C) Western blotting analysis of Bax, CYC, and CASP3 expressions in the studied groups, with GAPDH as an internal control. (D) CASP3, CYC, and Bax optical density values in each group. * $p < 0.05$ and ** $p < 0.01$, vs control group. Mean \pm SEM was used for data presentation, $n = 6$ per group.

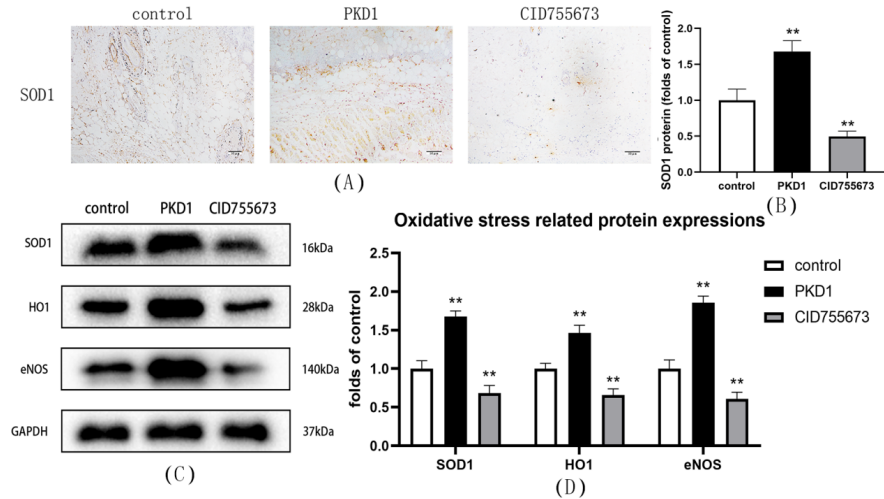


Figure 5: Effect of PKD1 on oxidative stress in the random-pattern skin flaps . (A) IHC staining of SOD1 expression in the flap in the studied groups (original magnification: 200×; scale bar: 50 μm). (B) The optical density values of SOD1 in the studied groups. (C) Western blotting analysis of SOD1, eNOS, and HO1 expressions in the studied groups, with GAPDH as an internal control. (D) HO1, SOD1, and eNOS optical density values in all groups. ** $p < 0.01$, vs control group. Mean \pm SEM was used for data presentation, $n = 6$ per group.